12-hydroxystearic acid-mediated in-situ surfactant generation: A novel approach for organohydrogel emulsions

Anne-Laure Fameau, Fabrice Cousin, Illia Dobryden, Clemence Dutot, Clémence Le Coeur, Jean-Paul Douliez, Sylvain Prévost, Bernard P Binks, Arnaud Saint-Jalmes

Journal of Colloid and Interface Science 672 (2024) 133–141

Contents lists available at ScienceDirect

Journal of Colloid And Interface Science

journal homepage: www.elsevier.com/locate/jcis

Regular Article

12-hydroxystearic acid-mediated *in-situ* surfactant generation: A novel approach for organohydrogel emulsions

Anne-Laure Fameau [a,*], Fabrice Cousin [b], Illia Dobryden [c], Clémence Dutot [d], Clémence Le Coeur [b,e], Jean-Paul Douliez [f], Sylvain Prevost [g], Bernard P. Binks [h], Arnaud Saint-Jalmes [d,*]

[a] University of Lille, CNRS, INRAE, Centrale institut, UMR 8207 - UMET - Unité Matériaux et Transformations, Lille, 59000, France
[b] Laboratoire Léon Brillouin, CEA, Saclay, France
[c] RISE Research Institutes of Sweden, Drottning Kristinas väg 61, 114 28 Stockholm, Sweden
[d] Université de Rennes, CNRS, IPR (Institut de Physique de Rennes), UMR 6251, Rennes, France
[e] CNRS, ICMPE, UMR 7182, 2 rue Henri Dunant, Université Paris Est Creteil, 94320 Thiais, France
[f] Biologie du Fruit et Pathologie, UMR 1332, Institut National de Recherche Agronomique (INRAE), Université de Bordeaux, Villenave d'Ornon F-33140, France
[g] Institut Laue-Langevin, 71 Avenue des Martyrs, CS 20156, Cedex 9, 38042 Grenoble, France
[h] Department of Chemistry, University of Hull, Hull HU6 7RX, UK

GRAPHICAL ABSTRACT

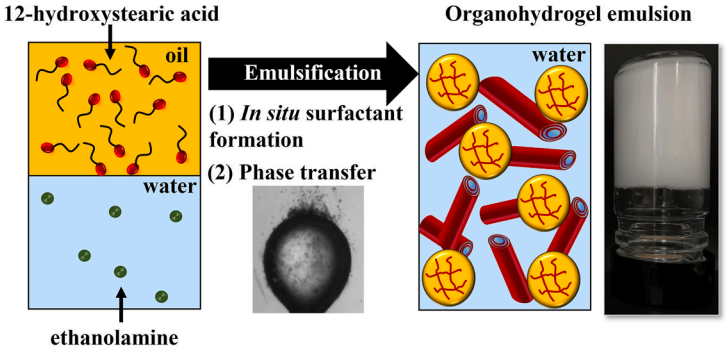

ARTICLE INFO

Keywords:
Gel emulsion
Hydrogelator
Organogelator
Phase transfer
Low energy process

ABSTRACT

Hypothesis: Organohydrogel emulsions display unique rheological properties and contain hydrophilic and lipophilic domains highly desirable for the loading of active compounds. They find utility in various applications from food to pharmaceuticals and cosmetic products. The current systems have limited applications due to complex expensive formulation and/or processing difficulties in scale-up. To solve these issues, a simple emulsification process coupled with unique compounds are required.

Experiments: Here, we report an organohydrogel emulsion based only on a low concentration of 12-hydroxystearic acid acting as a gelling agent for both oil and water phases but also as a surfactant. The emulsification process is based on *in-situ* surfactant transfer. We characterize the emulsification process occurring at the nanoscale by using tensiometry experiments. The emulsion structure was determined by coupling Small Angle X-ray and neutron scattering, and confocal Raman microscopy.

* Corresponding authors.
E-mail addresses: anne-laure.fameau@inrae.fr (A.-L. Fameau), arnaud.saint-jalmes@univ-rennes1.fr (A. Saint-Jalmes).

https://doi.org/10.1016/j.jcis.2024.05.213
Received 15 April 2024; Received in revised form 22 May 2024; Accepted 28 May 2024
Available online 29 May 2024

Findings: We demonstrate that the stability and unique rheological properties of these emulsions come from the presence of self-assembled crystalline structures of 12-hydroxystearic acid in both liquid phases. The emulsion properties can be tuned by varying the emulsion composition over a wide range. These gelled emulsions are prepared using a low energy method offering easy scale-up at an industrial level.

1. Introduction

Gel emulsions combine the virtues of both emulsions and gels [1]. They have garnered substantial interest in recent years [2]. Much like traditional emulsions, these gel emulsions constitute two-phase systems, with one phase dispersed as droplets in the other. However, they also show the characteristics of a physical gel. Consequently, gel emulsions display unique rheological behavior making them versatile and applicable across a wide range of fields including foods, cosmetics, drug delivery, tissue engineering and the fabrication of advanced porous materials [1,3–8]. One key advantage for applications is their high stability against the mechanisms that lead to emulsion destabilization, namely droplet coalescence and gravity-induced phase separation [9].

In 1966, Lissant *et al.* first defined gel emulsions to describe high internal phase emulsions (HIPEs) where the volume fraction of the dispersed phase can exceed 74 % [10]. Beyond this limit, droplets tend to deform adopting a polyhedral morphology [11]. HIPEs are renowned for their high elasticity, resulting from the compression of the droplets, and their high stability [9]. However, HIPEs have inherent limitations including the restricted range for adjusting the ratio of the two immiscible liquids (high dispersed phase volume fractions are required) leading to formulation constraints and the substantial quantity of stabilizer required which can be unsuitable for industrial processes notably in the food and cosmetic sector [8,9]. One innovative strategy that addresses the limitations of traditional HIPEs is the use of low molecular weight gelators (LMWGs) to gel the continuous phase of an emulsion yielding gel emulsions [12]. Such LMWGs are amphiphilic molecules that have the capability to self-assemble into fibrillar networks, effectively immobilizing organic solvents (organogel) or water (hydrogel) [2,13,14]. With LMWGs, the gelation mechanism that drives the formation of gel emulsions does not any longer rely on the packing of the dispersed droplets permitting a continuous tuning of the dispersed phase-to-continuous phase volume ratio. The success of such an approach is however dependent on the way the LMWGs self-assemble themselves, which is sensitive to parameters such as concentration, system composition, temperature and the nature of the immiscible liquids [12]. A further elegant extension of such a strategy is the dual-structured gelled emulsion, also called organohydrogel emulsion, for which both the water and oil phases are gelled simultaneously. To date, this innovative approach has been achieved however with the use of two different LMWGs – one for the aqueous phase and another for the oil phase [14]. The preparation process of organohydrogel emulsions contains two key steps: high energy emulsification followed by *in-situ* gelation.

To the best of our knowledge, there remains an unexplored frontier for the design of gel emulsions, where an "all-in-one" single molecule can serve at the same time as the stabilizing surfactant, the organogelator and the hydrogelator. Herein, we demonstrate that the formation of organohydrogel emulsions can be achieved using 12-hydroxystearic acid (12-HSA) as the only LMWG building block molecule. 12-HSA is a well-established LMWG, which can self-assemble into both organogels and hydrogels [15]. Its specific chemical structure gives rise to a plethora of self-assembled structures including fibres, ribbons and tubes depending on the medium conditions [15]. 12-HSA soaps also display

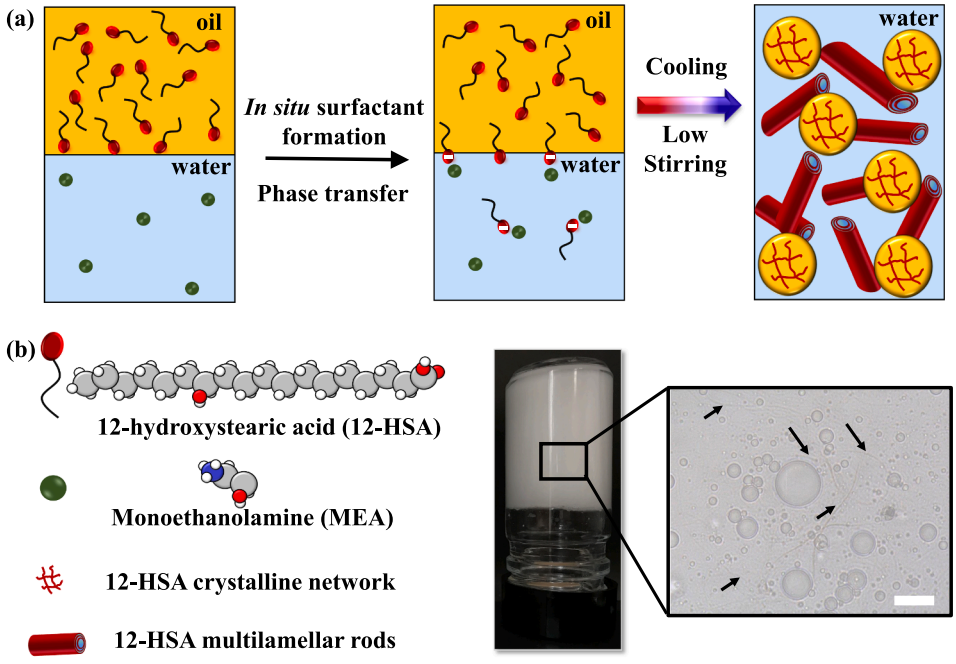

Fig. 1. *In situ* surfactant generation method used to produce organohydrogel oil-in-water emulsions. (a) Schematic illustration of emulsion gel based on *in situ* surfactant formation by phase transfer of 12-hydroxystearic acid from oil to water. 12-HSA and MEA were previously dissolved in oil and water at 80 °C, respectively. When the water and the oil phases were put in contact with low stirring, phase transfer of 12-HSA from oil to water occurs leading to surfactant formation and emulsification. During cooling, 12-HSA forms a self-assembled fibrillar network in the oil phase and micron size multilamellar rods in the water phase leading to both oil and water gelation. (b) Chemical structures of 12-HSA and MEA. (c) Gel emulsion obtained from the standard formulation (30 % v/v with *n*-dodecane as oil, 20 mM 12-HSA and 4 mM MEA in water) composed of oil droplets and 12-HSA multilamellar tubes denoted by the black arrows.

remarkable interfacial behavior giving rise to low surface tension while forming elastic interfacial layers [16–18]. Indeed, 12-HSA combined with other surfactants have already been used to produce gelled bicontinous microemulsions and gelled nanoemulsions [19,20].

Our approach to create organohydrogel emulsions relies on a low energy emulsification method known as the *in-situ* surfactant generation approach [21]. Such an approach involves generating a surfactant at the oil–water interface through gentle mixing of an organic phase containing a fatty acid and an aqueous alkaline phase [22–26]. We thus combine the *in-situ* surfactant generation approach with slow mixing to produce oil-in-water emulsions, and design dual-gelled structured emulsions by inducing the formation of gels in the oil and water phases with 12-HSA as the only building block (Fig. 1). The phase transfer of 12-HSA from oil to water improves the emulsification process by increasing the amount of surfactant at the oil–water interface enabling stabilization of the oil droplets. The phase transfer phenomenon also leads to 12-HSA self-assembled structures in the water phase giving rise to hydrogel formation. Excess 12-HSA molecules that remain in the oil form the organogel. The cosmetic grade ingredients used in these organohydrogel emulsions, their mechanical properties, their high stability over a long time period and the low energy process used for their production make them a promising system at large scale production for cosmetics products [27].

2. Materials and methods

2.1. Materials

12-Hydroxystearic acid (>80 % purity, impurities include 15 % stearic acid and other fatty acids in small amount, Xilong Chemical Co. Ltd., China), monoethanolamine (≥99.5 %, Sigma Aldrich, France), D_2O (>99 %, Eurisotop, France), *n*-dodecane (≥99 %, Sigma Aldrich, France), liquid paraffin oil (Sigma Aldrich, France), silicone oil (poly (dimethylsiloxane) with a viscosity of 100cSt) (Sigma Aldrich, France), isopropyl myristate Kollicream® IPM (BASF, Germany), medium chain triglyceride oil Kollisolv® MCT70 (BASF, Germany), olive oil and colza oil (local supermarket, France) were all used as received. MilliQ water was used for all the experiments.

2.2. Emulsion preparation

12-HSA powder was weighed and then completely dissolved in the oil phase at 80 °C under magnetic stirring. MEA was added to Milli-Q water and heated to 80 °C under magnetic stirring. Emulsification of the two phases was performed at 80 °C at 1,000 rpm for 2 min (Turbotest equipped with a deflocculating propeller turbine, VMI Rayneri, France). Then, the emulsion was allowed to cool to room temperature by keeping the agitation at 1,000 rpm to promote gelation of both phases and the subsequent formation of the structured gel emulsions. All the emulsions were stored at room temperature before further characterization. The same protocol was used for *ex situ* emulsion production, the only difference was being that 12-HSA was added to the water phase with MEA instead of the oil phase.

2.3. Single drop technique

The experiments at a single drop scale were performed using a tensiometer (Tracker apparatus, Teclis Scientific, France). Due to differences in density between water and oil, the rising drop configuration was chosen by using a curved syringe allowing us to create an oil drop rising within a water phase. The water phase contained MEA at around 1 mM and the oil phase contained 12-HSA at 0.25 mM to ensure no gelation of the oil droplet. The size of the drop was 1 mm and the volume was around 10 μL. The interfacial tension was obtained by fitting the shape of the droplet to the Young-Laplace equation.

2.4. Characterization of gelled emulsions

Optical micrographs were taken with an Axioscope 5 microscope with an Axiocam 208 camera (Zeiss, Germany). Samples were placed on a glass slide and covered with a coverslip. Samples were observed at room temperature using a 40x magnification in phase contrast mode.

Rheological measurements were performed with an Anton Paar MCR301 rheometer using a plate-plate setup. The walls of the plates in contact with the samples were roughened to prevent slip. Temperature control was provided using a Peltier plate. The temperature ramp used for these experiments was 1 °C/min. An oscillatory frequency of 1 Hz and a strain of 1 % were applied to measure the variation of the elastic modulus (G') and viscous modulus (G") with temperature to determine the temperature at which the transition between the gel state and liquid state occurred. Under the oscillatory mode, amplitude and frequency sweeps were performed to measure *G'* and *G"* as a function of the strain amplitude, γ, at constant frequency, *f*.

Small-Angle Neutron Scattering (SANS) data were acquired on D22 at the Institut Laue-Langevin (Grenoble) (https://doi.ill.fr/10.5291/ILL-DATA.9-10-1747). The wavelength was fixed at 6.0 Å (relative FWHM 10 %), the rear detector was at 17.6 m from the sample and the front detector at 1.4 m with a 20° angle thus covering a continuous *q*-range of 2.3x10^{-3}–0.64 Å^{-1}. Data were reduced with the program Grasp v10.17, normalizing with monitor, subtracting the contribution from the empty cell taking into account noise from the measurement with a sintered $^{10}B_4C$ piece at the sample position and using for transmission the intensity from the attenuated direct beam. Samples were held in 1 mm optical path length flat quartz cuvettes. Samples were prepared using D_2O instead of pure water. The data were fitted using SASview software. The fitting model is detailed in the Supplementary Information.

Small-angle X-ray scattering (SAXS) and Wide-Angle X-ray Scattering (WAXS) experiments were carried out on a XEUSS 2.0 device (Xenocs, France). The instrument uses a micro-focused Cu-Kα source with a wavelength of 1.54 Å and a Pilatus3 detector (Dectris, Switzerland). The samples were loaded in thin quartz capillaries (optical path 1.5 mm, WJM-Glas/Müller, Germany). The experiments were performed at two different sample-to-detector distances: 1190 mm with a collimated beam size of 0.5 mm × 0.5 mm and 340 mm with a collimated beam size of 0.8 mm × 0.8 mm, to access a scattering wave vector q-range of 0.01 Å^{-1} to 1.8 Å^{-1}.

Confocal Raman microscopy and spectroscopy measurements were conducted using a WITec Alpha 300 RAS system (Oxford Instruments, Germany) equipped with a 532 nm excitation laser and a spectrometer diffraction grating of 600 l/mm. A 50X Zeiss LD EC Epiplan-Neofluar Dic 50x/NA 0.55 and a Nikon CFI Plan NCG 100x/NA 0.9 objectives were used in this study. Laser power was optimized to minimize heat induced effects and was 15–20 mW. In the CRM mapping, a Raman spectrum is recorded in every image pixel. The typical compound spectra and their distribution are then identified using WITec Project Plus 5.1 software and the reconstructed Raman maps for all individual compounds and combined map are created. The identification is further verified using the measured reference spectra on individual compounds. All spectra were analysed with applied standard cosmic ray removal and baseline correction filters.

The estimation of the concentration of 12-HSA in the aqueous phase after emulsification was performed first by measuring the pH of the aqueous phase and by estimating the maximum number of molecules of 12-HSA that can react with MEA molecules in the acid-base reaction assuming a stoichiometric reaction of one molecule of 12-HSA reacting with one molecule of MEA. This quantity of 12-HSA in water was also estimated by weighing after destabilization of the emulsion by strong centrifugation and drying the aqueous phase.

2.5. Application of gelled emulsions

The moldability of the gelled emulsions was demonstrated by

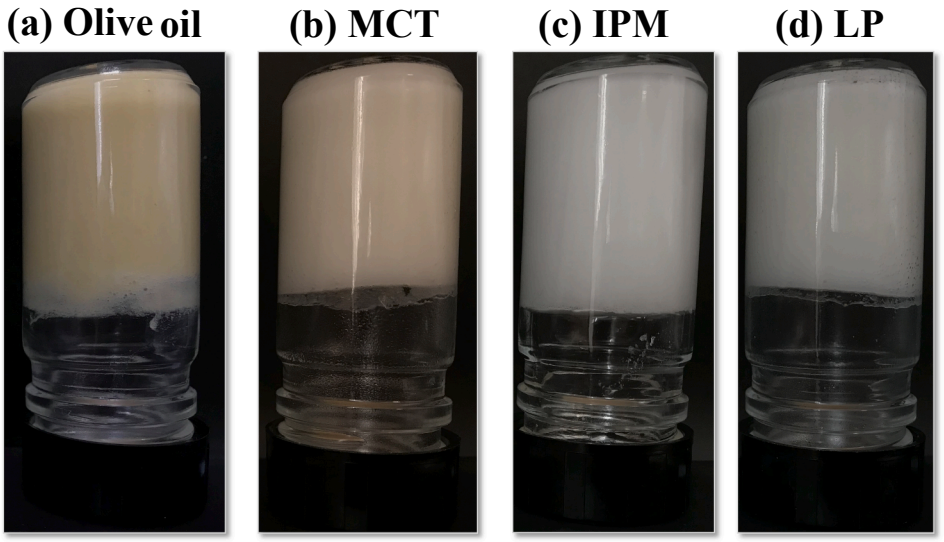

Fig. 2. Effect of oil type on gel emulsion formation: Photos of oil-in water emulsions (inverted) prepared from the standard formulation (30 % v/v oil and 20 mM 12-HSA) with different oils: (a) Olive oil, (b) medium chain triglyceride (MCT), (c) isopropyl myristate (IPM) and (d) liquid paraffin (LP).

fabricating 3D objects by injecting emulsions into different moulds. The gel emulsion was also used as a printable ink by loading it into a 12 mL syringe fitted with a needle (nozzle size of 0.51 mm). For the foamulsion production, a total volume of 15 mL of oil (30 % v/v) containing 20 mM of 12-HSA and water containing MEA at 4 mM were put directly at 80 °C in a 50 mL cylindrical plastic container (Falcon tube 50 mL, internal diameter 2.5 cm, 11.5 cm in height). A one-step aeration process by hand-shaking was used at high temperature for 5 min to produce the foam and emulsion at the same time.

3. Results and discussion

3.1. Organohydrogel emulsion formation

In order to demonstrate proof of concept of the formation of an organohydrogel emulsion by the use of only 12-HSA, we chose to work first with *n*-dodecane as a model oil. We first started with a low volume oil fraction (30 % v/v). Then we extended to other oils and oil volume fractions as shown later. To emulsify the oil phase in the aqueous phase, 12-HSA at 20 mM (with respect to the entire emulsion) was first dissolved in the oil phase at 80 °C (above the solubility limit) and monoethanolamine (MEA) counterion at 4 mM was added to the water phase heated at 80 °C. We fixed the molar ratio (R) between 12-HSA and MEA, $R = n_{MEA}/n_{12\text{-}HSA} = 0.2$, in order to obtain gel emulsions. This standard formulation was used for further characterization and understanding of the emulsion properties. At higher R, liquid emulsions were obtained (Supplementary Fig. 1). The pH of the aqueous phase was 10.3, higher than the apparent pK_a of 12-HSA and pK_b of MEA [28]. The oil-in-water emulsion was produced at 80 °C using the *in-situ* surfactant production method under low stirring, also called "slightly interfacial disturbance method" [21]. This process involved the instantaneous transfer of 12-HSA from oil to the water phase when the two phases were put into contact (Fig. 1a). The generation of the surfactant soap (anionic) form of 12-HSA occurred at the oil–water interface due to the neutralisation of 12-HSA with positively charged ($-NH_3^+$) MEA as a water-soluble base (Fig. 1b). Upon cooling, the 12-HSA remaining in the oil droplets crystallized leading to organogel droplets. The 12-HSA in the water phase self-assembled to form long rods and fibrillar structures of tens of micrometers in length giving rise to the gelation of the continuous phase (Fig. 1a). After emulsification, the pH of the water phase decreased to around 8.5. The pH was close to the apparent pKa of 12-HSA meaning that 12-HSA in the water phase was present in both its carboxylic (COOH) and soap (COO^-) forms [29]. The formed emulsion was an organohydrogel emulsion which can sustain its own weight (Fig. 1c). The average droplet diameter was around 2 μm as determined by Small Angle Neutron Scattering (SANS) (Supplementary Fig. 2). This low energy method only requires mixing at low stirring rate and gives rise to small droplets [21]. This process also offers the feasibility of large-scale production of the formulation [27].

To show the essential roles of both 12-HSA as building block and MEA, we conducted several control experiments. First, we pre-formed the 12-HSA soap by mixing 12-HSA and MEA directly in the water phase (pH around 8.5) at 80 °C before adding the oil phase. We call this process "*ex situ*", since the surfactant was produced before emulsification. A gel emulsion was formed but creaming occurred quickly and the droplet size was around 2.25 times bigger than the droplets produced by the *in-situ* process (Supplementary Fig. 2). Then, we replaced 12-HSA by stearic acid (SA), a fatty acid with the same alkyl chain length but without an –OH group on the 12th carbon. No stable gel emulsion was produced (Supplementary Fig. 3) [30]. Moreover, the nature of the counter-ion affects the self-assembled structure, solubility and interfacial properties of fatty acid soaps. We thus replaced MEA by sodium hydroxide as counter-ion and no emulsion could be produced (with Na^+ as counter-ion, formation of micron-sized crystals prevents the formation and stabilization of the emulsion) (Supplementary Fig. 4) [31]. The Krafft temperature is too high with sodium as counter-ion in comparison to MEA, leading to fast 12-HSA crystallization before the emulsion could be efficiently stabilized [32]. However, it is possible to use other organic amino counter-ions such as lysine and choline hydroxide known to decrease the Krafft temperature of fatty acid soaps instead of MEA [33]. For both choline hydroxide and lysine as counter-ion, stable gel emulsions were obtained showing the robustness of 12-HSA as a unique building block for the easy production of gel emulsions (Supplementary Fig. 5). We demonstrated the universality of our approach to produce stable gel emulsions by studying a variety of other oils including vegetable oils, medium chain triglyceride (MCT), isopropyl myristate (IPM) and liquid paraffin (LP) (Fig. 2).

3.2. Low energy emulsification process coupled with surfactant phase transfer

To assess our hypothesis regarding the underlying mechanism at the interface leading to an optimized emulsification process combined with hydrodynamical fragmentation, we performed experiments at the scale

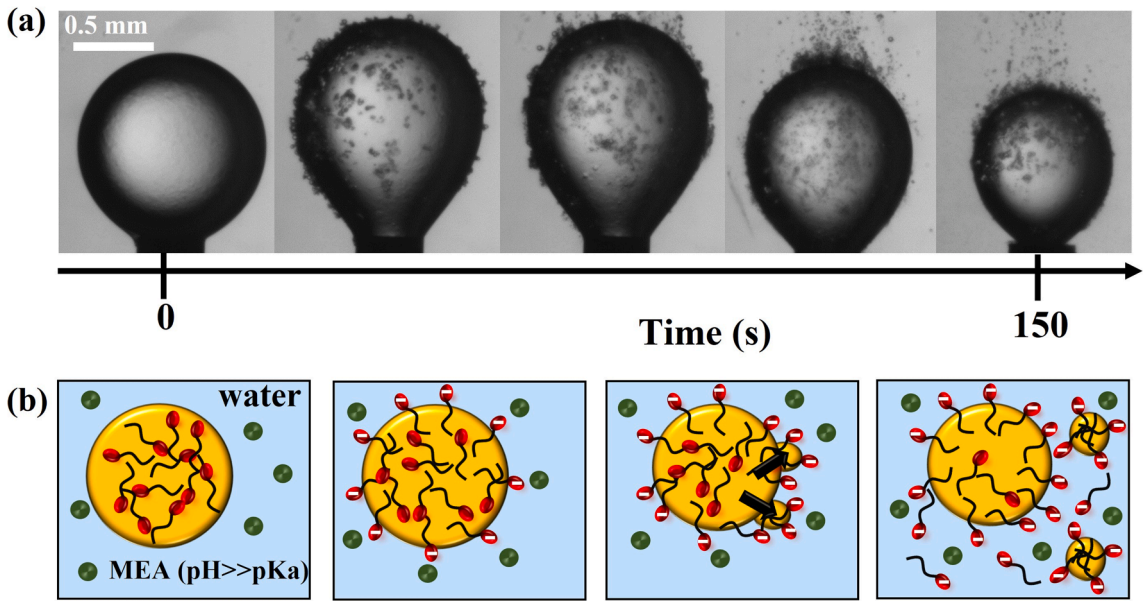

Fig. 3. Low energy emulsification process by surfactant phase transfer. (a) Evolution with time of a drop of MCT oil containing 12-HSA in water containing MEA (pH > pK_a). The photos were taken every 20–30 *sec*. (b) Schematic showing the fragmentation of the initial oil droplet into smaller droplets due to the transfer of 12-HSA across the interface. Negatively charged 12-HSA surfactant molecules were formed at the interface stabilizing the newly formed oil droplets.

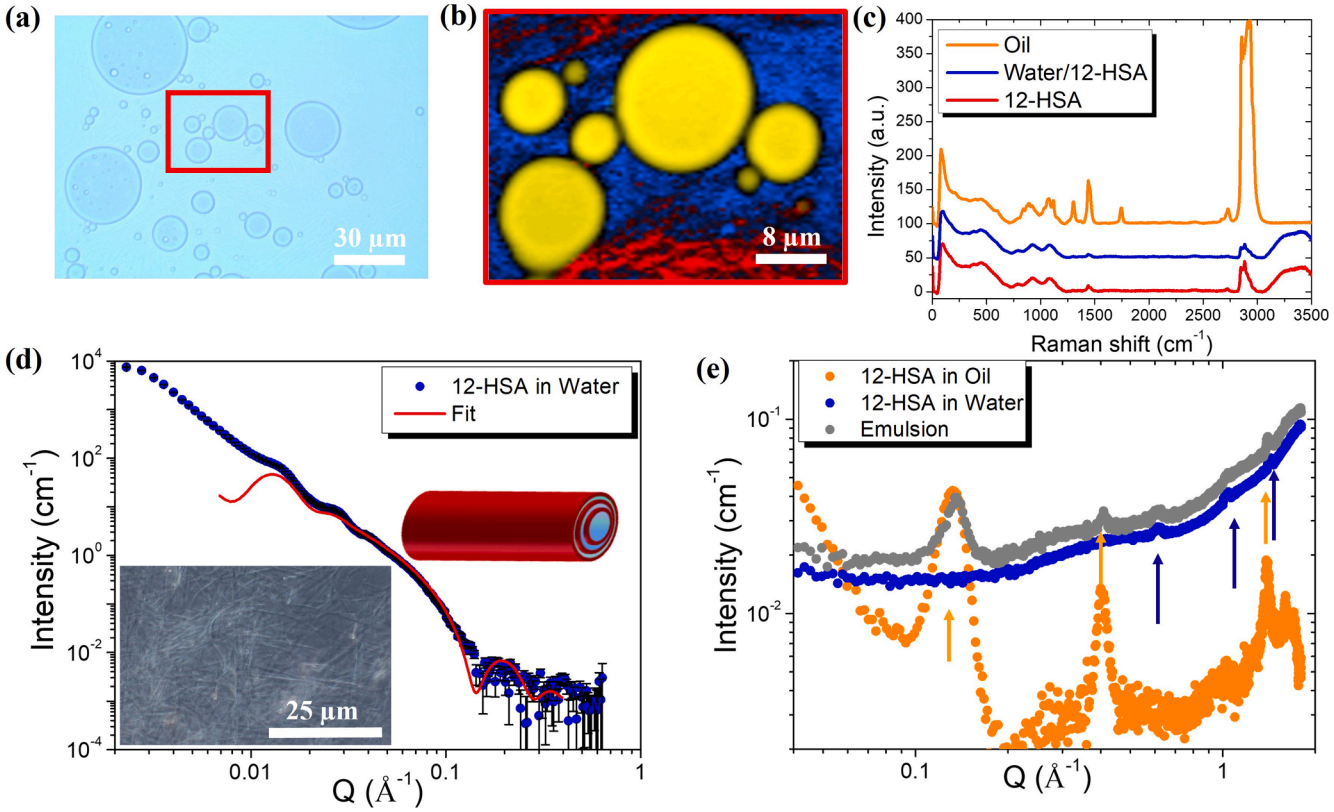

Fig. 4. Structural characterization of gel emulsions. (a) Optical image of a gel emulsion (standard formulation with 30 % v/v MCT oil and 20 mM 12-HSA) where a confocal Raman map inside the red rectangle was measured. (b) Combined Raman map demonstrating distribution of three main components ((yellow) oil, (red) clustered 12-HSA in water and (blue) water/HSA) as obtained by analysing Raman spectra for each pixel of image. (c) Corresponding Raman spectra identified in the measured Raman map and used to reconstruct the component distribution maps. The color code in the spectra and Raman map is the same. (d) SANS spectrum of the aqueous phase of 20 mM of 12-HSA with MEA with the corresponding phase contrast microscopy image showing the presence of multilamellar rods and fibers. (e) SAXS spectra of: (orange) 20 mM 12-HSA in MCT oil after subtraction of the contribution of pure MCT oil, (blue) 20 mM 12-HSA with 4 mM MEA in water, (grey) emulsion based on 20 mM 12-HSA in MCT oil and 4 mM MEA in water. (For interpretation of the references to color in this figure legend, the reader is referred to the web version of this article.)

of one single oil drop in water using the rising drop method. A millimeter drop of oil (MCT) containing 2 mM of 12-HSA (a concentration sufficiently low to avoid oil gelation) was held at the tip of a syringe surrounded by water. In the presence of 12-HSA in oil, but without MEA in the water phase, the interfacial tension was stable with time at 23.3 mN m^{-1} slightly lower than the interfacial tension between pure oil and water (24.2 mN m^{-1}). However, immediately after adding MEA to the water phase leading to an alkaline solution (pH ≫ pK_a), the drop divided into smaller droplets leaving the initial drop (Fig. 3a and Supplementary Movie 1). The same findings have been obtained with different oils (Supplementary Fig. 6). Small droplets were created at the interface and a self-sustaining stream of droplets detached from the interface. The interfacial tension of the initial drop also decreased to reach a low value around 4.5 ± 1.5 mN m^{-1}. This interfacial tension is similar to the one obtained between neat oil and the aqueous phase containing 12-HSA and MEA (*ex-situ* process). This demonstrates that the interface of the drop was covered by 12-HSA under its surface-active ionised form. The reaction that occurred at the interface led to *in-situ* surfactant production (Fig. 3b). As long as it remains in the oil phase, 12-HSA is in its uncharged state. However, when surrounded by a water phase containing MEA (alkaline solution, pH > pK_a), it migrates by diffusion onto the droplet surface where the headgroups are deprotonated and transformed into their surface-active form (carboxylate/soap form) facing the aqueous phase (Fig. 3b). The neutralization reaction between 12-HSA and MEA quickly creates a non-equilibrium, high density interfacial layer resulting in the low interfacial tension measured. This interfacial reaction led to interfacial disturbance being the origin of oil fragmentation into small droplets. These interfacial disturbances come from the combination of surfactant transfer across the interface and the subsequent flows induced inside and outside the droplets in response to surface tension gradients (Marangoni effect) [21]. Locally, the concentration of 12-HSA soap at the interface can become so high (corresponding to very low interfacial tension) that any perturbation can grow and overcome the stabilizing effect of interfacial tension. In the single drop experiment, gravity amplifies this perturbation (replaced by viscous shear stresses during mixing) which eventually induce droplet separation as the Plateau-Rayleigh instability tends to break the connecting liquid bridges [34]. Therefore, an initial millimeter single droplet fragments into a multitude of smaller ones leading to an emulsion with micron sized droplets. The process could continue until all 12-HSA in the oil phase is depleted. It could be also halted due to 12-HSA crystallization induced by cooling or when the pH of the water phase becomes too low (<pK_a). The emulsification process by mixing is thus enhanced by the *in-situ* surfactant generation process.

Moreover, by studying the same interface with an optical microscope under a planar configuration, we observed that the interfacial reaction also led to surfactant transfer of 12-HSA from the oil phase to the water phase. It was possible to follow the growth of 12-HSA self-assembled fibres leaving the oil droplets (Supplementary Movie 2 and Supplementary Figure 7). Thus, the *in-situ* surfactant formation at the interface led to both emulsification and droplet stability against coalescence (electrostatic repulsion) and the creation of 12-HSA self-assembled structures in the water phase.

3.3. Stabilization mechanism and emulsion structure

The origin of the stability of the gel emulsions was studied at different length scales by combining confocal Raman microscopy (CRM), wide-angle X-ray scattering (WAXS) and SANS experiments. CRM was carried out to obtain the distribution image of the different components within the emulsion at the micron scale. First, the Raman spectra of the reference compounds oil, water and 12-HSA were measured to determine the specific bands associated with each compound (Supplementary Figure 8). In Fig. 4a, the red frame placed in the optical image of the gel emulsion indicates the area where the Raman mapping was measured. The reconstructed Raman map for combined signals from oil, water and 12-HSA is shown in Fig. 4b-c. The superposition of the three images using color-coding clearly shows the presence of a high amount of self-assembled 12-HSA aggregates in the aqueous phase (Supplementary Figure 8). The oil spectra correlate well with the reference spectra *e.g.* as characterized by a clear presence of 1744 cm^{-1} carbonyl C═O band (Supplementary Figure 8). The distribution of 12-HSA was confirmed by a specific CH-stretching shape with two characteristic peak locations at 2848 cm^{-1} and 2884 cm^{-1}. Also, OH-bands with two characteristic peak locations in the range of 3200 cm^{-1}-3400 cm^{-1} were observed and could be assigned to water molecules. The red signal in the Raman map indicated higher concentration of 12-HSA and could be assigned to the formed larger self-assembled structures of 12-HSA, as suggested by stronger CH-stretching band intensity ratio to the OH-band compared to the blue signal. Thus, application of confocal Raman microscopy allowed visualization of oil and the 12-HSA self-assembled structure dispersed in water. The CRM lateral resolution was limited by the applied laser wavelength and of the objective, and thus it could not resolve and detect nanosized self-assembled 12-HSA structures in oil.

To probe the gelled emulsion to obtain structural information at the nanoscale, we combined SAXS and SANS. However, it was impossible to determine the 12-HSA self-assembled structures by SANS in the emulsion since its scattered intensity is completely dominated by the Q^{-4} Porod scattering decay of the droplets (Supplementary Fig. 2). To gain insight into the 12-HSA self-assembled structure in the water phase, we studied instead an aqueous dispersion containing 20 mM of 12-HSA with MEA that corresponds to the limiting case where all 12-HSA molecules would transfer to the water phase (Fig. 4d). Optical microscopy showed that the continuous phase contains long 12-HSA rods and fibers. On the SANS spectrum Fig. 3d, there is a Bragg peak at $Q_0 = 0.014$ $Å^{-1}$ followed by two harmonics at $2Q_0$ and $3Q_0$ that demonstrates the formation of a lamellar phase showing that 12-HSA self-assembles into multilamellar rods and fibers. The position of the Bragg peaks was associated with the interlamellar distance (*d*-spacing) at intermediate *Q* with an oscillation at $Q \sim 0.2$ $Å^{-1}$ originating from the lamella form factor at large *Q*. At large *Q*, there is an oscillation at $Q \sim 0.2$ $Å^{-1}$ originating from the lamella form factor. The scattering curve was fitted in the intermediate and large *Q* region *via* a model proposed by Nallet *et al.* to determine the structural parameters of lamella (thickness, *d*-spacing and rigidity) (Supplementary Information Note S6)[35]. This model takes into account the form factor of the lamella and the structure factor coming from the lamellas (number of stacked bilayers and the thermal fluctuations of the bilayers defined by the Caillé parameter (η)) [35]. It allows a good fitting of the SANS scattered intensity showing that the 12-HSA molecules do form lamellar phases with 5 layers on average and a *d*-spacing of 455 Å. η was equal to 0.005 showing rigid lamella with a thickness of 45 ± 1 Å corresponding to 12-HSA molecules self-organized into a gel crystalline β phase [28]. Thus, when the 12-HSA has transferred from the oil droplets, it self-assembles into micron-size multilamellar 12-HSA aggregates in water.

Then we used WAXS on emulsions to probe the formation of 12-HSA crystalline structures inside both the aqueous and oil phases (Fig. 4e). The diffractogram showed the presence of several correlation and Bragg peaks that we compared to those of two reference samples, respectively pure 12-HSA in oil and an aqueous solution of 12-HSA with MEA (Fig. 4e). The three peaks of 12-HSA in water (0.619, 1.02 and 1.45 Å) confirmed the presence of crystallized 12-HSA in the water phase. These peaks are characteristic of the crystalline structure of 12-HSA inside the lamella of multilamellar rods [31]. For 12-HSA in the oil phase, four peaks were evidenced at 0.133, 0.397, 1.39 and 1.61 Å that are characteristic of 12-HSA molecules aggregated in double-plane layers forming long fibers in accordance with literature [36–38]. It turns out that all peaks coming from the crystalline structure of 12-HSA in the oil phase and in the water phase were recovered on the emulsion diffractogram. It is proof that 12-HSA not only self-assembles in the water phase but 12-HSA also remains in the oil droplets as a crystalline self-

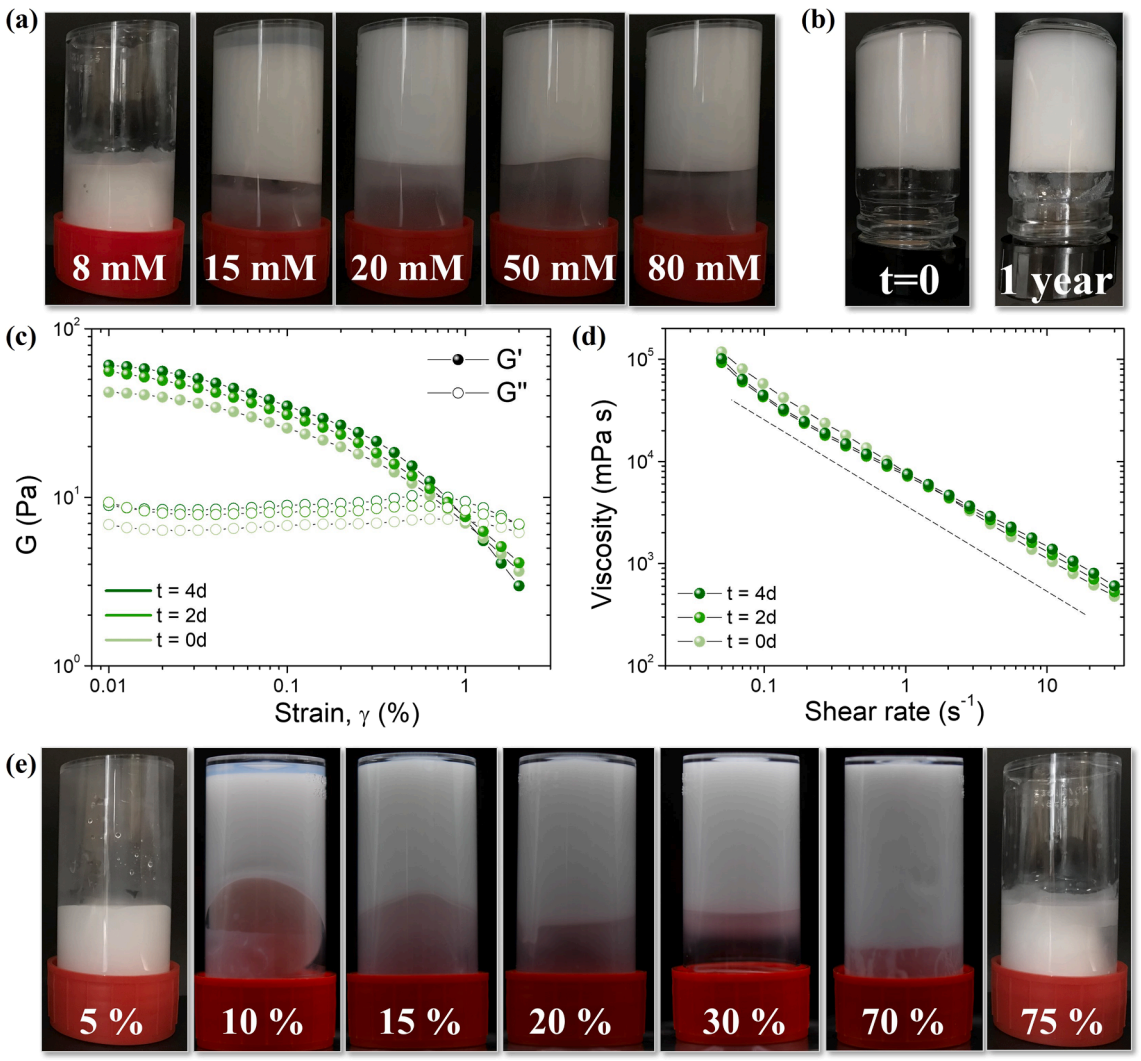

Fig. 5. Formulation, stability and rheological properties of gel emulsions. (a) Photos of 30 % v/v dodecane-in-water emulsion (inverted) at different 12-HSA concentrations from 8 to 80 mM. (b) Photos of gel emulsion (inverted) at 20 mM 12-HSA with dodecane after emulsion production (t = 0) and after one year of storage at room temperature. (c) Strain amplitude sweep and (d) steady-state flow curve for a gel emulsion (30 % v/v MCT and 20 mM 12-HSA) at different times in days at room temperature. The dashed line in (d) is a power law with an exponent −0.7 indicating the scaling behavior at high shear rates. (e) Photos of dodecane-in water emulsions (inverted) prepared at a constant concentration of 12-HSA = 20 mM but with different oil volume fractions as indicated.

assembled structure. The same conclusions were obtained when the oil in the emulsion is liquid paraffin (Supplementary Figure 10). It is important to recognise that a possible growing of the 12-HSA structure could happen with time depending on the oil and the formulation used [37].

3.4. Organohydrogel emulsion versatility, stability and rheological properties

Next we studied the effect of 12-HSA concentration, with respect to the overall emulsion, on the emulsifying ability of 30 % v/v *n*-dodecane. Below 20 mM surfactant, a fluid emulsion or a gel emulsion exhibiting creaming were observed (Fig. 5a) whereas stable gel emulsions were obtained up to 80 mM. We estimate that the concentration of 12-HSA in the aqueous phase after emulsification was 4 mM (0.12 wt%) for a concentration of 20 mM of 12-HSA in the whole emulsion, *i.e.* the lowest enabling gel emulsion formation. This concentration is lower than the ones reported for the most efficient LMWGs to produce a gel emulsion (5 mM/0.2 wt% for dehydroabietic acid derivative although the gel emulsion shows creaming)[2]. Furthermore, we did not take into account the 12-HSA at the interface; it is thus likely that the concentration in the water phase is indeed even lower. The formed organohydrogel emulsion also offered a long shelf-life and remained stable for at least one year at room temperature as shown in Fig. 5b and the standard formulation could resist high centrifugal forces (Supplementary Figure 11). We determined the rheological properties of the emulsion produced using our standard formulation (oil volume fraction 30 %) (Fig. 5c, d). There was a range of low amplitude where the elastic modulus (G') is higher than the viscous one (G"), indicating a solid-like behavior. Then, at higher amplitudes, the emulsions started to flow above a yield point and viscosity eventually dominates elasticity. The mechanical behavior did not evolve with ageing since it was reproducible after several days of storage of the emulsion at room temperature. Such behaviour was also observed for the gel emulsion based on liquid paraffin (Supplementary Figure 12). The transition from a gel emulsion to a liquid one was followed by rheological measurements, and the gel emulsions were stable for a wide range of temperature until 77 °C for liquid paraffin and 68 °C for MCT (Supplementary Figure 13). Their complex modulus then decreases by almost 2 orders of magnitude at this threshold temperature since emulsions were completely destabilized. This threshold temperature corresponds to the melting point of 12-HSA that leads to the disappearance of the gel network in the oil and water phases

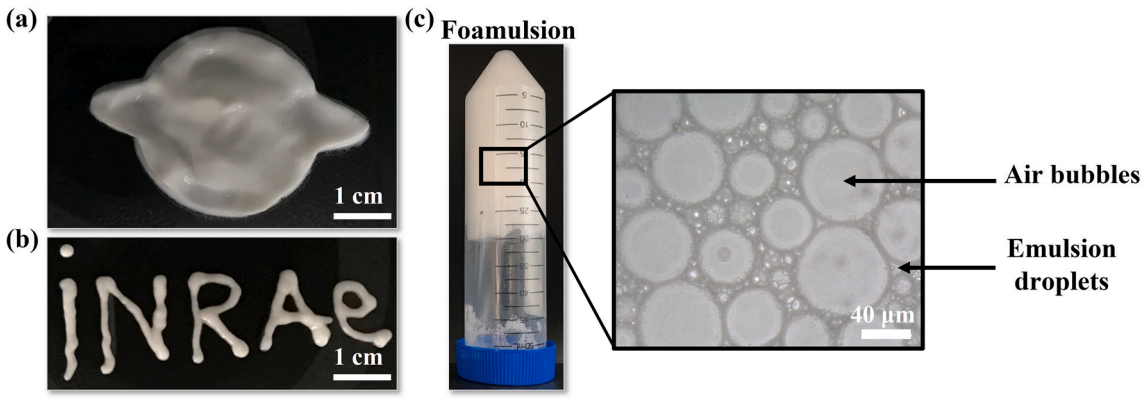

Fig. 6. Versatility of organohydrogel emulsions. (a) Photo' of an object shaped after 1 h from the standard formulation emulsion based on 20 mM 12-HSA in *n*-dodecane by using a mold. (b) Same emulsion as in (a) was used for writing letters by extrusion through a needle showing the processability of the gel emulsion. Photo' taken 1 day after generation. (c) Photo' of an inverted foamulsion produced by handshaking the standard formulation used in (a). The corresponding optical microscopy image shows that air bubbles are surrounded by emulsion droplets.

(Supplementary Figure 14). The excellent long-term stability was attributed to both the gelled continuous aqueous phase and the gelled oil dispersed phase preventing flocculation and coalescence of the droplets with time. Moreover, the flow curve of the emulsions showed a strong shear-thinning behavior as demonstrated by the dependence of the viscosity as a function of shear rate ($\eta \sim \gamma^{-m}$ with $m = 0.7$) encountered classically for HIPEs but not for emulsions at low oil volume fraction (Fig. 5d)[8].

We also studied the effect of oil volume fraction in emulsions containing 20 mM 12-HSA. At low volume fraction (5 %), a liquid emulsion was obtained. However, at 10 % oil a gel emulsion was formed which exhibited some creaming. Stable gel emulsions were obtained for oil volume fractions from 15 % to 70 % showing that emulsion gels could be obtained for a wide range of oil volume fraction even if some systems exhibited a wider range [2].

We took advantage of the excellent stability and unique viscoelastic properties of the organogel emulsions to test their processability. We showed that these emulsions were moldable materials by creating stable 3D object with a mold and could be extruded with a nozzle (Fig. 6a-b and Supplementary Figure 15). To show that these gel emulsions could also serve to build more complex structured multiphase systems, we studied the production of emulsion foams or foamulsion by air incorporation [39]. Foamulsion was easily produced as illustrated in Fig. 6b and was stable for at least 1 month (Supplementary Figure 16). The high foam stability was mainly attributed to the highly viscoelastic hydrogel network in the continuous phase as well as the clogging of the oil droplets in the liquid channels.

4. Conclusion

For the first time, we experimentally demonstrate that organohydrogel emulsions can be produced by surfactant transfer which aids emulsification by using 12-hydroxystearic acid as the only building block. This chemical engineering approach not only helps to produce the emulsion droplets stabilized by surfactant but also leads simultaneously to the formation of self-assembled structures of 12-HSA in the water phase and in the oil phase. 12-HSA formed both organogel droplets and gelled the water phase. This enhances the emulsion stability even at low oil volume fraction and low 12-HSA concentration. Unlike previous research on organohydrogel emulsions based on LMWGs, each of which requires a high energy emulsification process and two components to gel the oil and water phases, our method is applicable to various oils with a wide range of polarity and to a large range of oil:water ratios[12]. We also demonstrated that it was possible to create foamulsions of high stability in which air bubble surfaces are covered by 12-HSA surfactant molecules. The organohydrogel emulsions shown here for 3-D printing and inks could have several advantages in comparison to traditional inks, since both water-soluble and organic-soluble components could be included into these emulsions which could give rise to new functionalities[5]. Our organohydrogel emulsions have already been used to create hair coloration cream at large scale for cosmetic applications leading to a facile, fast and environmentally friendly process (decrease of energy consumption) [27]. We therefore expect that these novel gel emulsion systems could also be used for a broader range of sustainable applications in foods, pharmaceuticals and biological fields and also for the design of functional materials [5,40].

Funding

This research was funded by INRAE TRANSFORM department.

CRediT authorship contribution statement

Anne-Laure Fameau: Writing – review & editing, Writing – original draft, Validation, Project administration, Methodology, Investigation, Formal analysis, Data curation, Conceptualization. **Fabrice Cousin:** Writing – review & editing, Investigation, Formal analysis, Conceptualization. **Illia Dobryden:** Writing – review & editing, Methodology, Investigation. **Clémence Dutot:** Writing – review & editing, Investigation, Formal analysis. **Clémence Le Coeur:** Writing – review & editing, Investigation, Formal analysis. **Jean-Paul Douliez:** Writing – review & editing, Conceptualization. **Sylvain Prevost:** Methodology, Investigation. **Bernard P. Binks:** Writing – review & editing, Validation, Methodology, Conceptualization. **Arnaud Saint-Jalmes:** Writing – review & editing, Validation, Supervision, Project administration, Methodology, Investigation, Funding acquisition, Formal analysis, Conceptualization.

Declaration of competing interest

The authors declare that they have no known competing financial interests or personal relationships that could have appeared to influence the work reported in this paper.

Data availability

Data will be made available on request.

Acknowledgements

This work benefited from the use of the SasView application originally developed under NSF award DMR-0520547. SasView contains code developed with funding from the European Union Horizon 2020

research and innovation program under the SINE2020 project, grant agreement No 654000.

Appendix A. Supplementary data

Supplementary data to this article can be found online at https://doi.org/10.1016/j.jcis.2024.05.213.

References

[1] S.M. Hashemnejad, A.Z.M. Badruddoza, B. Zarket, C. Ricardo Castaneda, P. S. Doyle, Thermoresponsive nanoemulsion-based gel synthesized through a low-energy process, Nat. Commun. 10 (2019) 2749.

[2] T. Yan, B. Song, X. Pei, Z. Cui, B.P. Binks, H. Yang, Widely adaptable oil-in-water gel emulsions stabilized by an amphiphilic hydrogelator derived from dehydroabietic acid, Angew, Chemie. 132 (2020) 647–651.

[3] B. Wu, C. Yang, Q. Xin, L. Kong, M. Eggersdorfer, J. Ruan, P. Zhao, J. Shan, K. Liu, D. Chen, Attractive Pickering emulsion gels, Adv. Mater. 33 (2021) 2102362.

[4] Y. Zhu, S. Huan, L. Bai, A. Ketola, X. Shi, X. Zhang, J.A. Ketoja, O.J. Rojas, High internal phase oil-in-water pickering emulsions stabilized by chitin nanofibrils: 3D structuring and solid foam, ACS Appl. Mater. Interfaces. 12 (2020) 11240–11251.

[5] S. Huan, B.D. Mattos, R. Ajdary, W. Xiang, L. Bai, O.J. Rojas, Two-phase emulgels for direct ink writing of skin-bearing architectures, Adv. Funct. Mater. 29 (2019) 1902990.

[6] D. Lin, A.L. Kelly, S. Miao, Preparation, structure-property relationships and applications of different emulsion gels: Bulk emulsion gels, emulsion gel particles, and fluid emulsion gels, Trends Food Sci. Technol. 102 (2020) 123–137.

[7] N. Brun, S. Ungureanu, H. Deleuze, R. Backov, Hybrid foams, colloids and beyond: From design to applications, Chem. Soc. Rev. 40 (2011) 771–788.

[8] A.M.B. Rodriguez, B.P. Binks, High internal phase Pickering emulsions, Curr. Opin. Colloid Interface Sci. 57 (2022) 101556.

[9] T. Farjami, A. Madadlou, An overview on preparation of emulsion-filled gels and emulsion particulate gels, Trends Food Sci. Technol. 86 (2019) 85–94.

[10] K.J. Lissant, The geometry of high-internal-phase-ratio emulsions, J. Colloid Interface Sci. 22 (1966) 462–468.

[11] T.G. Mason, J. Bibette, D.A. Weitz, Elasticity of compressed emulsions, Phys. Rev. Lett. 75 (1995) 2051.

[12] Z. Zhang, J. Hao, Bioinspired organohydrogels with heterostructures: Fabrications, performances, and applications, Adv. Colloid Interface Sci. 292 (2021) 102408.

[13] J. Peng, H. Xia, K. Liu, D. Gao, M. Yang, N. Yan, Y. Fang, Water-in-oil gel emulsions from a cholesterol derivative: Structure and unusual properties, J. Colloid Interface Sci. 336 (2009) 780–785.

[14] J. Chen, Q. Li, R. Du, X. Yu, Z. Wan, X. Yang, Thermoresponsive Dual-Structured Gel Emulsions Stabilized by Glycyrrhizic Acid Nanofibrils in Combination with Monoglyceride Crystals, Molecules. 27 (2022) 6542.

[15] A.-L. Fameau, M.A. Rogers, The curious case of 12-hydroxystearic acid — the Dr. Jekyll & Mr. Hyde of molecular gelators, Curr. Opin. Colloid Interface Sci. 45 (2020) 68–82.

[16] A.-L. Fameau, A. Saint-Jalmes, F. Cousin, B. Houinsou Houssou, B. Novales, L. Navailles, F. Nallet, C. Gaillard, F. Boué, J.-P. Douliez, Smart foams: Switching reversibly between ultrastable and unstable foams, Angew. Chemie - Int. Ed. 50 (2011) 8264–8269.

[17] K.S. Yim, B. Rahaii, G.G. Fuller, Surface rheological transitions in Langmuir monolayers of bi-competitive fatty acids, Langmuir. 18 (2002) 6597–6601.

[18] D. Vollhardt, S. Siegel, D.A. Cadenhead, Effect of hydroxyl group position and system parameters on the features of hydroxystearic acid monolayers, Langmuir. 20 (2004) 7670–7677.

[19] M. Laupheimer, K. Jovic, F.E. Antunes, M. da G.M. Miguel, C. Stubenrauch, Studying orthogonal self-assembled systems: Phase behaviour and rheology of gelled microemulsions, Soft Matter. 9 (2013) 3661–3670.

[20] V. Nouri, M.P.D.S. Moura, B. Payre, O. De Almeida, C. Déjugnat, S. Franceschi, E. Perez, How an organogelator can gelate water: gelation transfer from oil to water induced by a nanoemulsion, Soft Matter. 16 (2020) 2371–2378.

[21] D. Cholakova, Z. Vinarov, S. Tcholakova, N.D. Denkov, Self-emulsification in chemical and pharmaceutical technologies, Curr. Opin. Colloid Interface Sci. 59 (2022) 101576.

[22] J.W. McBain, T.-M. Woo, Spontaneous emulsification, and reactions overshooting equilibrium, Proc. R. Soc. London. Ser. A-Mathematical Phys. Sci. 163 (1937) 182–188.

[23] U. El-Jaby, M. Cunningham, T.F.L. McKenna, The advantages of in situ surfactant generation for miniemulsions, Macromol. Rapid Commun. 31 (2010) 558–562.

[24] U. El-Jaby, M. Cunningham, T.F.L. McKenna, Miniemulsions via in situ Surfactant Generation, Macromol. Chem. Phys. 211 (2010) 1377–1386.

[25] J. Chatterjee, D.T. Wasan, A kinetic model for dynamic interfacial tension variation in an acidic oil/alkali/surfactant system, Chem. Eng. Sci. 53 (1998) 2711–2725.

[26] B.B. Niraula, T.N. Seng, M. Misran, Vesicles in fatty acid salt–fatty acid stabilized o/w emulsion—emulsion structure and rheology, Colloids Surfaces A Physicochem. Eng. Asp. 236 (2004) 7–22.

[27] S.-K. Koudedji, K. Wunsch, A. Camblong, A.-L. Fameau, Composition comprising 12-hydroxystearic acid, an organic amine and a liquid fatty substance, PCT/EP2020/068091. WO2020260629A1, 2020.

[28] A.-L. Fameau, F. Cousin, A. Saint-Jalmes, Morphological Transition in Fatty Acid Self-Assemblies: A Process Driven by the Interplay between the Chain-Melting and Surface-Melting Process of the Hydrogen Bonds, Langmuir. 33 (2017).

[29] J.R. Kanicky, A.F. Poniatowski, N.R. Mehta, D.O. Shah, Cooperativity among molecules at interfaces in relation to various technological processes: effect of chain length on the p K a of fatty acid salt solutions, Langmuir. 16 (2000) 172–177.

[30] A.-L. Fameau, B. Houinsou-Houssou, B. Novales, L. Navailles, F. Nallet, J.-P. Douliez, 12-Hydroxystearic acid lipid tubes under various experimental conditions, J. Colloid Interface Sci. 341 (2010).

[31] A.-L. Fameau, T. Zemb, Self-assembly of fatty acids in the presence of amines and cationic components, Adv. Colloid Interface Sci. 207 (2014) 43–64.

[32] W. Kunz, P. Lo Nostro, B.W. Ninham, The present state of affairs with Hofmeister effects, Curr. Opin. Colloid Interface Sci. 9 (2004) 1–18.

[33] R. Klein, D. Touraud, W. Kunz, Choline carboxylate surfactants: biocompatible and highly soluble in water, Green Chem. 10 (2008) 433–435.

[34] B.A. Grzybowski, Reaction-Driven Mixing and Dispersion, Angew. Chemie Int. Ed. 1 (2010) 40–42.

[35] F. Nallet, R. Laversanne, D. Roux, Modelling X-ray or neutron scattering spectra of lyotropic lamellar phases: interplay between form and structure factors, J. Phys. II (3) (1993) 487–502.

[36] P. Terech, Small-angle-scattering study of 12-hydroxystearic physical organogels and lubricating greases, Colloid Polym. Sci. 269 (1991) 490–500.

[37] M.A. Rogers, A.J. Wright, A.G. Marangoni, Crystalline stability of self-assembled fibrillar networks of 12-hydroxystearic acid in edible oils, Food Res. Int. 41 (2008) 1026–1034.

[38] Y. Lan, M.G. Corradini, R.G. Weiss, S.R. Raghavan, M.A. Rogers, To gel or not to gel: correlating molecular gelation with solvent parameters, Chem. Soc. Rev. 44 (2015) 6035–6058.

[39] A. Salonen, Mixing bubbles and drops to make foamed emulsions, Curr. Opin. Colloid Interface Sci. 50 (2020) 101381.

[40] L. Bai, S. Huan, O.J. Rojas, D.J. McClements, Recent innovations in emulsion science and technology for food applications, J. Agric. Food Chem. 69 (2021) 8944–8963.